LANGMUIR Article
Cite This: Langmuir 2020, 36, 789−795
pubs.acs.org/Langmuir

In Situ Seed-Mediated Growth of Polymer-Grafted Gold Nanoparticles

Yu-Xi Wang,[†,#] Ai-Ju Li,[†,#] He-Lei Wang,[‡,#] Wei Liu,[§] Jing Kang,[†] Jun Lu,[†] Shao-Yong Lu,[†] Yang Yang,[†,∥] Kun Liu,*[,†,∥] and Bai Yang[†,∥]

[†]State Key Laboratory of Supramolecular Structure and Materials, College of Chemistry, Jilin University, Changchun 130012, P. R. China

[‡]Department of Gastrointestinal Surgery, The First Hospital of Jilin University, Changchun 130000, P. R. China

[§]School of Materials Science and Engineering, Shaanxi Key Laboratory of Green Preparation and Functionalization for Inorganic Materials, Shaanxi University of Science & Technology, Xi'an,710021, P. R. China

[∥]State Key Laboratory of Applied Optics, Changchun Institute of Optics, Fine Mechanics and Physics, Chinese Academy of Sciences, Changchun 130012, P. R. China

Supporting Information

ABSTRACT: We report a facile yet general in situ seed-mediated method for the synthesis of polymer-grafted gold nanoparticles with narrow size distributions (<10%), accurately tunable sizes, and excellent colloidal stability. This method can be extended to a broad range of types and molecular weights of polymer ligands. Nanoparticles with different shapes can also be prepared by using preformed shaped nanoparticles directly as the seeds.

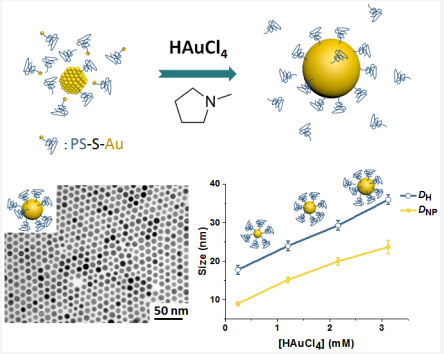

Polymer-grafted nanoparticles (NPs),[1−3] in which polymer ligands are covalently attached onto an inorganic nanoparticle surface, have drawn considerable attention from both fundamental research and practical application fields.[4−13] The polymer component can serve as either steric stabilizer in solution and in polymer matrix to prevent the agglomeration of the attached nanoparticles and/or functional linker to control the structure and collective properties of the assembly of nanoparticles.[14−19] Therefore, it is critical to develop efficient preparation methods for monodisperse polymer-grafted nanoparticles with controllable grafting density, uniform grafting density distribution, low polydispersity index (PDI) of polymer ligands, and excellent colloidal stability.

Generally, there are two complementary methods for the preparation of polymer-grafted nanoparticles, that is, "grafting-from"[20−26] and "grafting-to"[27−42] methods with each technique possessing unique merits and disadvantages.[43−45] The "grafting-from" method involves polymerization of monomer directly from initiator-functionalized nanoparticle surfaces. This method easily allows for high grafting densities to be achieved; however, it provides less uniformity of polymer coverage on the NP surface and poor PDI of the synthesized polymer ligands. In contrast, in the "grafting-to" process, end-functionalized polymer ligands are grafted onto the surface of existing NPs via the replacement of small molecular ligands used for the synthesis of NPs. This method has the advantage of using preformed well-defined polymers with known molecular architectures, predetermined molecular weights, and narrow polydispersity, resulting in more uniform grafting density distributions.[45] The "grafting-to" method typically suffers from inability to achieve high grafting densities because of two reasons: (1) polymer chains must diffuse through the existing grafted polymer layer to react with the NP surface, and (2) it is difficult for polymer ligands to replace small molecule ligands more densely packed on the NP surface.[46]

Another less common approach, the "in situ" method (sometimes also categorized as "grafting-to" method),[47−50] is to directly use a well-defined polymer as a stabilizing reagent in the synthesis of core NPs without the presence of small molecule ligands.[49] Therefore, higher grafting density (compared to that of the grafting-to method), better PDI, and polymer coverage uniformity can be achieved, resulting in an excellent colloidal stability. However, the size distribution of the as-prepared NPs, e.g., gold NPs (GNPs), is often difficult to control (polydispersity over 20%), and only relatively small

Received: November 15, 2019
Revised: December 6, 2019
Published: December 9, 2019

DOI: 10.1021/acs.langmuir.9b03542
Langmuir 2020, 36, 789−795

GNPs (diameters less than 10 nm) can be obtained,[10,51,52] which is not comparable to those of well-established preparation methods of GNPs. These issues severely hinder the development of this method.

Herein we report a facile yet general in situ seed-mediated method for the synthesis of polymer-grafted GNPs with narrow size distributions (<10%). Gold seeds with sizes below 2 nm in aqueous solution are synthesized following a highly reproducible method described previously. The gold seeds are transferred to tetrahydrofuran (THF) for the growth of spherical GNPs with thiol-terminated polystyrene (PS-SH, M_n = 4200 g/mol) ligands and 1-methylpyrrolidine (1-MPR) as a mild reducing agent. The size of the produced PS-grafted GNPs (GNP@PS) can be accurately fine-tuned from 9.0 ± 0.5 to 23.7 ± 1.8 nm depending on the regrowth steps (i.e., gold precursor to seed ratio). PS-SH with different molecular weights (4200 to 40000 g/mol) shows negligible effect on the size and size distribution of the resulting GNP@PS but can be used to control their hydrodynamic radius. Importantly, the GNP@PS prepared by the in situ seed-mediated method shows better colloidal stability than that prepared by the "grafting-to" method with the same size of GNPs and molecule weight of PS-SH ligands. We also demonstrate that the in situ seed-mediated method is applicable for the synthesis of GNPs with other polymer ligands, such as thiol-terminated poly(ethylene glycol) (PEG-SH), thiol-terminated poly(2-(dimethylamino)ethyl methacrylate) (PDMAEMA-SH), thiol-terminated poly(methyl methacrylate) (PMMA-SH) in ethanol, deionized water (DI water), and THF, respectively. This method can be extended for the preparation of polymer-grafted GNPs with other shapes, e.g., PS-grafted gold nanorods (GNR@PS) by using preformed gold nanorods (GNRs) as the seeds.

Seed-mediated synthesis of NPs is one of the most frequently used methods for producing metal NPs such as Au, Ag, Pd, or Cu NPs, with well-controlled shapes, sizes, and size distribution.[53] In a seed-mediated method, the formation of seeds (i.e., metal clusters or small NPs) and the growth of NPs from these seeds are separated into two distinct stages, so that the formation of new seeds in the second (growth) stage is suppressed. Deposition on the existing nucleus has an energy barrier lower than that of formation of a new nucleus, which makes seed-mediated growth method favorable for a narrow size distribution of NPs.[55] For example, in the case of the synthesis of GNRs in water,[54] cetyltrimethylammonium bromide (CTAB)-stabilized gold cluster seeds with sizes below 2 nm are prepared by reducing Au(III) to Au(0) with a strong reducing agent (sodium borohydride), while further formation of seeds in the second stage (growth solution) is inhibited by using a weak reducing agent (ascorbic acid) that can only reduce Au(III) to Au(I). Therefore, all the seeds are formed at the same time in the first stage and grew under identical conditions in the second stage, resulting GNRs with narrow size distributions.[55]

The preparation of gold cluster seeds in the method mentioned above is highly reproducible, and their growth mechanism has been well studied. In addition, Vaia and co-workers[56] reported that the gold cluster seeds can be phase-transferred from water into nonpolar solvents, such as toluene and THF, in the presence of PS-SH, which binds strongly to the gold seed surface by Au−S bonds. Therefore, we choose to use the CTAB-covered gold cluster seeds for the synthesis of GNP@PS.

For the growth solution, chloroauric acid ($HAuCl_4$) in THF (0.24 mM) as the precursor of Au was reduced by 1-MPR (40 mM) in the presence of PS-SH (M_n = 4200 g/mol, PDI = 1.04, 0.40 mM) (see details for the preparation of thiol-terminated polymers by reversible addition−fragmentation chain transfer (RAFT) polymerizations in Figures S1 and S2, and Tables S1 and S2). The concentration of PS-SH (0.40 mM) was found to be a critical concentration for synthesizing the GNP@PS. Below 0.40 mM, the surface plasmonic band (between 600 to 700 nm) for the aggregates of GNPs was observed in the extinction spectra (Figure S3). The color of the solution changed from light yellowish to colorless within 2 min after the addition of 1-MPR, indicating that gold ions were only reduced from Au(III) to Au(I) and no gold clusters (brownish color) or GNPs (reddish color) were observed. The Au(I) ions were stabilized by the formation of a Au(I)-S-PS complex, which was the precursor for the growth of Au nanoparticles.[57] Without addition of external gold cluster seeds, the growth solution turned to brown-pink color only after 10 h. This result suggests that although 1-MPR can reduce Au(III) to Au(0), the self-nucleation of gold seeds in the growth solution is very slow. In contrast, introducing the gold cluster seeds (40 μL) into the freshly prepared growth solution (2 min after the addition of 1-MPR) resulted in a color change of the solution to reddish in 30 min at room temperature, indicating the much faster formation of GNPs. The growth of GNP@PS was continued over 10 h. TEM study of the produced GNP@PS (Figure 1a) shows an average diameter of the gold core (D_{NP})

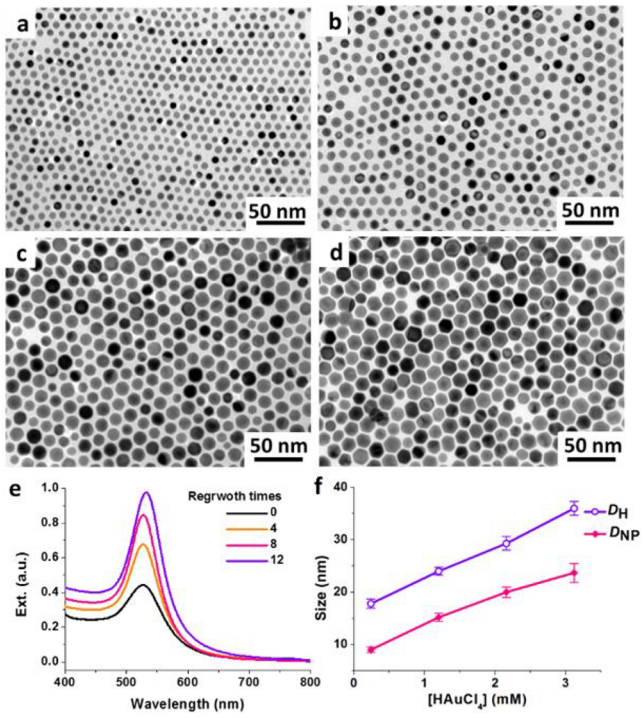

Figure 1. TEM images of GNP@PS synthesized by PS-SH (M_n = 4200 g/mol) with different regrowth times for various average diameters of the gold core (D_{NP}): (a) regrowth 0 times and D_{NP} = 9.0 ± 0.5 nm, (b) regrowth 4 times and D_{NP} = 15.2 ± 0.8 nm, (c) regrowth 8 times and D_{NP} = 20.0 ± 1.0 nm, (d) regrowth 12 times and D_{NP} = 23.7 ± 1.8 nm. (e) Extinction spectra of GNP@PS with different regrowth times. (f) The plot of the D_{NP} and hydrodynamic diameters (D_H) of the corresponding GNP@PS with the accumulated concentration of $HAuCl_4$ used for regrowth.

DOI: 10.1021/acs.langmuir.9b03542
Langmuir 2020, 36, 789−795

Scheme 1. Growth Mechanism of Polymer-Grafted Au Nanoparticles

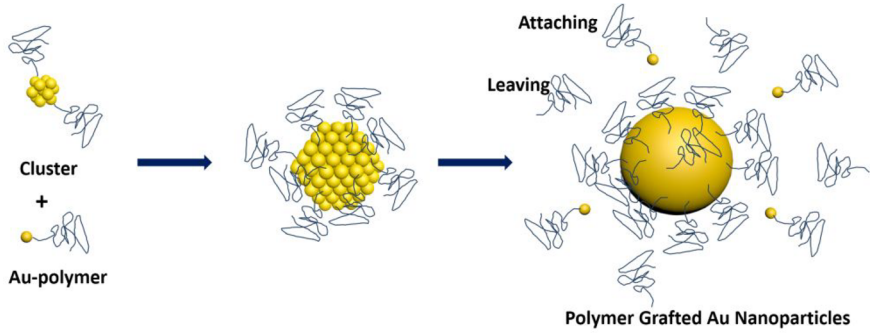

of 9.0 ± 0.5 nm with a standard deviation less than 10% (Figure S4). The GNP@PS displayed a localized surface plasmon resonance (LSPR) peak at 528 nm with a relatively narrow full width of half-maximum (fwhm) of 60 nm (Figure 1e).

It is indeed interesting that thiol-terminated polymer ligands allow for the growth of relatively larger nanoparticles while only gold clusters or small nanoparticles (in general with size less than 5 nm) can be obtained by using small molecular alkanethiols as the ligand with otherwise identical conditions. There are two possible reasons for the difference: (1) the chemisorption of small molecular alkanethiols is rather strong due to the van der Waals force between the tightly packed alkane chains,[58] and the polymer chain was tethered onto the surface of GNPs by a dynamic covalent mechanism; (2) the grafting density of the polymer on the GNPs is lower than that of small molecule ligands. Therefore, the surface of GNPs or clusters is not completely terminated by polymer ligands, and the Au(I)-S-PS complexes can penetrate through the shell of polymer chains and deposit on the uncovered Au surface, resulting in growth of larger GNPs as illustrated in Scheme 1. In comparison, small molecular ligands with higher grafting densities hinder the growth of gold nanoparticles by preventing the deposition of gold atoms onto them.

The diameter of GNPs, i.e., D_{NP}, plays a key role in determining their plasmonic properties. A synthetic method capable of precise control of GNP diameters is strongly desired. We found that with the current in situ seed-mediated method, the D_{NP} of the produced GNP@PS can be accurately fine-tuned from 9.0 ± 0.5 nm to 23.7 ± 1.8 nm through continuous multiple regrowth steps. The key in each regrowth step is to control the concentration of Au(0) below their supersaturation concentration for the formation of new gold seeds; otherwise, both new and preformed seeds can grow, resulting in the formation of GNPs with diverse sizes and shapes.[57] In each step, a small amount of $HAuCl_4$ (0.24 mM) was added into the growth solution with the existing GNP@PS. This concentration of gold precursor was appropriate to prevent forming new seeds, and in the meantime high enough to deposit onto presynthesized gold seeds. The TEM analysis reveals that the increase of D_{NP} for each step was about 1 nm, and in the meantime the polydispersity was kept below 10% (Figure S5 and Table S3). More importantly, no new small GNPs were observed. Direct regrowth of GNP@PS from 9 to above 20 nm by the addition of a large amount of $HAuCl_4$ at once led to the formation of a new nucleus and broadening the size distribution as shown in Figure S6.

The multiple steps in the regrowth process were also monitored by using UV−vis spectroscopy and dynamic light scattering (DLS) as shown in Figure 1e,f and Table 1. As D_{NP} of GNP@PS increased from 9.0 ± 0.5 to 23.7 ± 1.8 nm, their LSPR peaks were red-shifted from 528 to 532 nm as expected, and fwhm was kept below 60 nm, which was consistent with the low polydispersity determined by TEM studies. The hydrodynamic diameters (D_H) of GNP@PS produced with different regrowth steps also confirmed their narrow size distributions. The increase of D_H was mainly attributed to the diameter increase of the inorganic core, i.e., D_{NP}, because the differences between D_H and D_{NP} were nearly constant, corresponding to the thickness of the PS shell.

Table 1. Seed-Mediated Growth of GNP@PS with Different Regrowth Steps by Using PS-SH (M_n = 4200 g/mol)

regrowth steps	D_{NP} (nm)	D_H (nm)	$HAuCl_4$[a] (mM)	LSPR (nm)	fwhm (nm)
0	9.0 ± 0.5	17.8 ± 0.9	0.24	528	60
4	15.2 ± 0.8	24.0 ± 0.8	1.20	528	54
8	20.0 ± 1.0	29.3 ± 1.3	2.16	530	54
12	23.7 ± 1.8	36.0 ± 1.3	3.12	532	56

[a]The concentration of the $HAuCl_4$ was the accumulated concentration.

Interestingly, as D_{NP} of the GNP@PS increased, their shape changed from sphere to faceted cuboctahedron, a Wulff equilibrium crystal polyhedron enclosed by 8 triangular (111) facets and 6 square (100) facets.[59] The shape evolution is favored by thermodynamics: as the D_{NP} of GNP@PS increases, the ratio of atoms at the faces (lower surface energy) to corners and edges (higher surface energy) increases; that is, the facets become more dominated. The high resolution TEM image as shown in Figure S7 proved that GNP@PS is single-crystalline, which is consistent with the GNRs and gold nanocubes synthesized from the same type of gold cluster seeds.[59]

To study the effect of molecular weight of PS-SH on GNP@PS, a series of PS-SH with M_n of 4200, 12700, 30200, and 40000 g/mol were utilized for the synthesis of GNP@PS with a fixed molar concentration of polymer chains (0.40 mM) and $HAuCl_4$ (0.60 mM) under otherwise identical conditions used for previous regrowth experiments. TEM studies of dry films of GNPs stabilized by PS-SH with different M_n (Figure 2a−d) reveal that the molecular weight of PS-SH has a negligible effect on the core size of GNPs and their narrow size distribution but clearly increased the interparticle distances in their dry films due to the thicker polymer shells for higher M_n of PS-SH (Table S4). A clear core−shell structure of GNP@PS synthesized with PS-SH (M_n = 40000 g/mol) can be observed

DOI: 10.1021/acs.langmuir.9b03542
Langmuir 2020, 36, 789−795

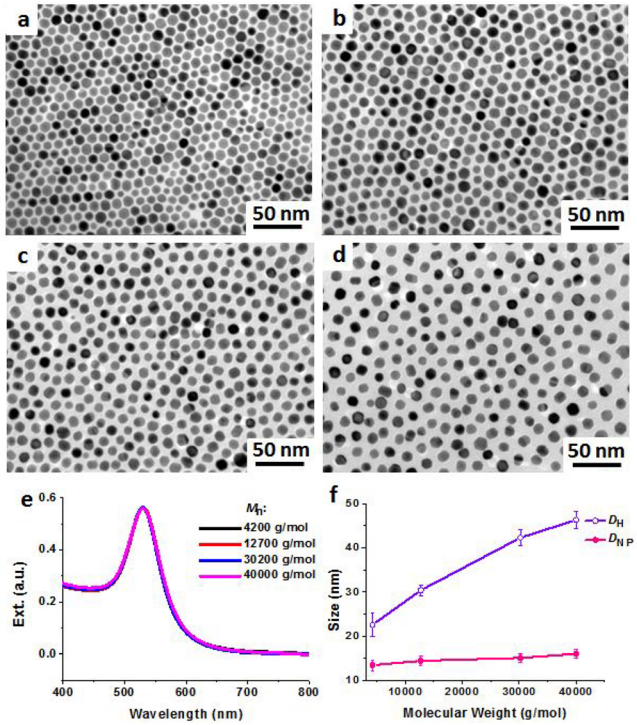

Figure 2. TEM images (a–d) showing the GNPs stabilized by PS with different molecular weights (0.4 mM). (a) M_n = 4200 g/mol and D_{NP} = 13.7 ± 1.0 nm, (b) M_n = 12700 g/mol and D_{NP} = 14.3 ± 0.9 nm, (c) M_n = 30200 g/mol and D_{NP} = 15.1 ± 0.9 nm, (d) M_n = 40000 g/mol and D_{NP} = 16.1 ± 1.0 nm. (e) Extinction spectra of GNP@PS with different molecular weights. (f) The plot of the D_{NP} and D_H of the corresponding GNP@PS with different molecular weights measured by TEM and DLS, respectively.

in the TEM image (Figure S8). The fact that the GNPs@PS with different M_n of PS-SH have similar sizes suggests that the reactivity of Au(I)-S-PS only slightly changed with M_n of PS-SH, which is consistent with the equal reactivity assumption for polymerization theory.[60] As shown in Figure 2e, the extinction spectra of the GNP@PS with different M_n were almost identical, and the fwhm of LSPR peaks were well controlled to be about 60 nm, indicating narrow size distributions of the produced GNPs with similar D_{NP}. As the D_{NP} of GNP@PS only slightly changed with M_n, the large increase of D_H determined by DLS was mainly attributed to the chain lengths of PS-SH ligands. (Figure 2f)

The colloidal stability of NPs plays a key role for their practical applications. To evaluate the colloidal stability of GNP@PS synthesized by the in situ seed-mediated method, we used grafting-to method to prepare PS grafted GNPs (GNP@PS*) with almost identical D_{NP} (15.3 ± 0.8 nm vs 15.4 ± 0.8 nm) by utilizing the same PS-SH solution (M_n = 4200 g/mol, 0.40 mM). The concentrations of the two types of GNP solutions were also adjusted to be almost the same (~2.2 nM). The colloidal stability was compared by repeated centrifugations (see experimental section in SI for details). The extinction spectra of two types of GNP solutions for different centrifugation cycles are shown in Figure 3. For GNP@PS* after three centrifugation cycles, the LSPR peak was red-shifted and broadened with less intensity, indicating the formation of GNP aggregation. In contrast, the extinction spectra of GNP@PS had no obvious changes even after five centrifugation cycles, suggesting that GNP@PS remained as individually

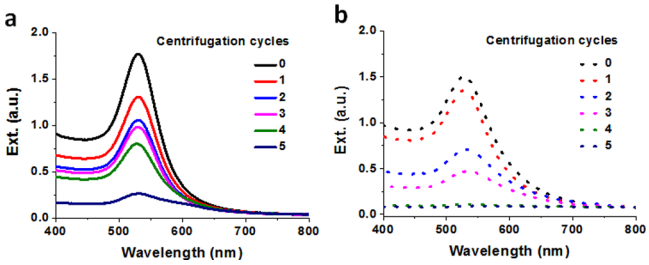

Figure 3. Extinction spectra of (a) the GNP@PS (D_{NP} = 15.4 ± 0.8 nm, 2.2 nM) with PS-SH (M_n = 4200 g/mol, 0.40 mM) after centrifugation 0–5 cycles. (b) Sodium citrate-protected GNPs (D_{NP} = 15.3 ± 0.8 nm, 2.2 nM) replaced by PS-SH (M_n = 4200 g/mol, 0.40 mM) after centrifugation 0–5 cycles.

dispersed in the solution. In addition, GNP@PS also performs better in thermal and chemical stability than that of GNP@PS*. As shown in Figure S9, GNP@PS* was aggregated within 90 min after being heated at 70 °C or the addition of oxidant *tert*-butyl hydroperoxide, while GNP@PS remained colloidally stable in the solution under identical conditions. GNP@PS prepared by the in situ seed-mediated method also showed a good long-term stability (>1 month) due to the steric effect of PS-SH ligands. These results suggest that the polymer-grafted nanoparticles prepared by the in situ seed-mediated method possess better colloidal stability compared to that by the grafting-to method. Indeed, the grafting density of GNP@PS prepared by the in situ seed-mediated method (0.36 chains/nm^2) was similar to that obtained by the "grafting-to method" (0.32 chains/nm^2) (Figure S10). The better colloidal stability should be attributed to the better uniformity of grafting density distribution.

Encouraged by the successful preparation of GNP@PS with controlled D_{NP} and ligand chain lengths, we tested a series of technically important polymer ligands, including PDMAEMA-SH (M_n = 7600 g/mol), PEG-SH (M_n = 5000 g/mol), and PMMA-SH (M_n = 7100 g/mol), to illustrate the generality of the in situ seed-mediated strategy. By using the same gold cluster seeds, GNP@PDMAEMA, GNP@PEG, and GNP@PMMA were synthesized in good solvents for each type of polymer ligand, i.e., DI water, ethanol, and THF, respectively. TEM image analysis (Figure 4a–c) shows that the produced GNP@PDMAEMA, GNP@PEG, and GNP@PMMA possessed D_{NP} of 7.5 ± 0.79, 9.8 ± 0.68, and 15.9 ± 1.5 nm, respectively, and have narrow size distributions with their polydispersity of 10% or even lower. The different sizes of the produced GNP@PDMAEMA, GNP@PEG, and GNP@PMMA could be attributed to the reactivity difference among the Au-polymer intermediates, that is Au(I)-S-PDMAEMA, Au(I)-S-PEG, and Au(I)-S-PMMA.

The corresponding extinction spectra also confirmed the similar narrow fwhm of about 60 nm comparable with those of GNP@PS (Figure 4d). These results suggest that the in situ seed-mediated strategy is not limited by the type of thiol-terminated polymer ligands or solvents and is therefore applicable for the preparation of polymer-grafted nanoparticles in a broad range. Interestingly, D_{NP} of GNP@PMMA was considerably larger than those of GNP@PEG and GNP@PDMAEMA, although the precursor concentration for PMMA (6.0 mM) was even lower (15.0 mM for PEG and PDMAEMA) with otherwise identical conditions, except for the solvent (see Synthesis of GNPs with Different Polymers in

DOI: 10.1021/acs.langmuir.9b03542
Langmuir 2020, 36, 789–795

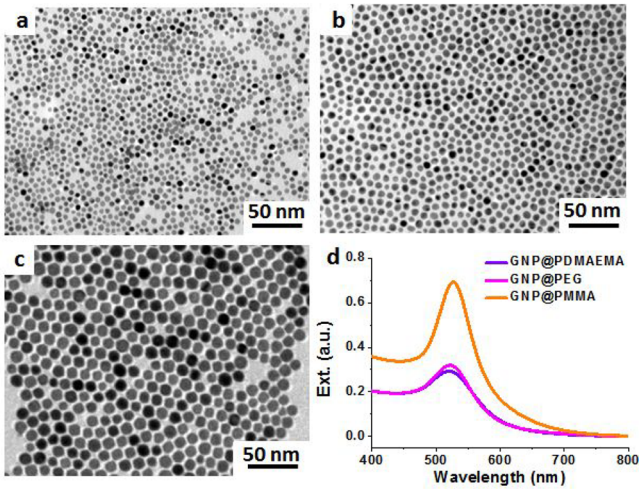

Figure 4. TEM images (a–c) of the GNPs synthesized by different polymer ligands: (a) PDMAEMA-SH (M_n = 7600 g/mol) and D_{NP} = 7.5 ± 0.79 nm, (b) PEG-SH (M_n = 5000 g/mol) and D_{NP} = 9.8 ± 0.68 nm, and (c) PMMA-SH (M_n = 7100 g/mol) and D_{NP} = 15.9 ± 1.5 nm. (d) Extinction spectra of GNP@PDMAEMA, GNP@PEG, and GNP@PMMA in DI water, ethanol, and THF, respectively.

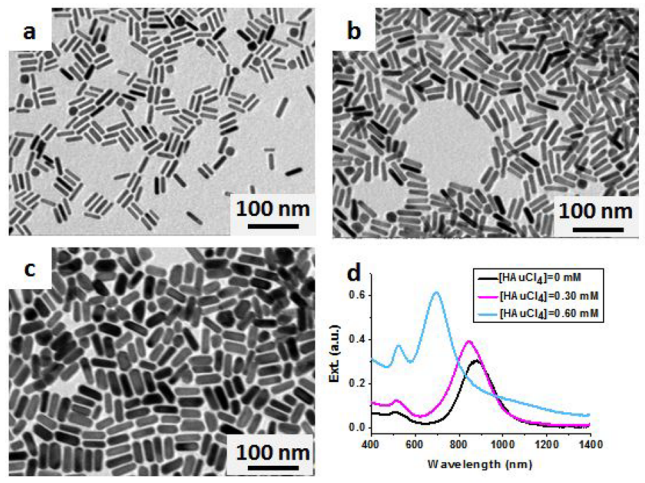

Figure 5. TEM images of the gold nanorods (GNRs) (a) stabilized by PS-SH in THF as seeds before growth and (b, c) after the growth with different concentrations of $HAuCl_4$: (b) [$HAuCl_4$] = 0.30 mM and (c) [HAuCl4] = 0.60 mM. (d) Extinction spectra of the GNR seeds transferred before and after the growth.

SI). This result indicates that the reactivity of Au(I)-S-polymer precursor could be affected by the structure of polymer chains.

We also extend this in situ seed-mediated strategy for the preparation of polymer-grafted nanoparticles with controlled shape by directly using preformed shaped GNPs, such as GNRs, as the seeds. CTAB-coated GNRs with an average length and width of 32.6 ± 3.6 and 7.7 ± 0.9 nm (Figure 5a), respectively, were synthesized in water following a highly reproducible protocol reported previously.[54] The presynthesized GNRs covered by CTAB were aggregated when added into THF, a poor solvent for CTAB. Instead, to prepare GNR@PS in THF solution, the GNRs were phase transferred from water into THF by using PS-SH through a ligand exchange process.[49] The GNR@PS in THF solution were used as seeds and added into the growth solution containing PS-SH (M_n = 4200 g/mol, 0.60 mM), $HAuCl_4$, and 1-MPR (20 mM). TEM images of the produced GNR@PS with different concentrations of $HAuCl_4$ are shown in Figure 5b,c. After the growth, the average length/width of the GNR@PS increased to 37.0 ± 5.4/9.6 ± 1.2 nm and then to 45.1 ± 1.8/15.9 ± 1.7 nm for the $HAuCl_4$ concentration of 0.30 and 0.60 mM, respectively. This result suggests that the gold precursor was deposited on both the end and side of the GNR@PS, and the average length/width of GNR@PS can be tuned by the amount of gold precursor without broadening their size distributions. In comparison with the extinction spectra of GNR@PS in THF before and after growth (Figure 5d), the longitudinal LSPR peak was blue-shifted from 875 to 698 nm, which also indicates the aspect ratio (the length to width ratio) of the GNR@PS became smaller.[61] These results demonstrate that the in situ seed-mediated growth method we developed can be used to synthesize polymer-stabilized GNPs with different shapes by varying the shape of the seeds.

In summary, we have demonstrated a general in situ seed-mediated strategy for the preparation of size- and shape-controlled polymer-grafted GNPs with narrow size distributions. The size of the produced GNP@PS can be accurately fine-tuned by the regrowth steps. The molecular weight of polymer ligands can be used to control their hydrodynamic radius of GNP@PS, while showing negligible effects on their size and size distribution. We also demonstrate that this method is applicable for the synthesis of GNPs with other polymer ligands and even GNPs with different shapes by using preformed shaped nanoparticles directly as the seeds. Importantly, the GNP@PS prepared by in situ seed-mediated method shows better colloidal stability than that prepared by "grafting-to" method. This strategy paves a new path for the synthesis of inorganic nanoparticles with controllable size, shape, narrow size distribution, and uniform polymer ligand density, which are important for their long-term colloidal stability and practical applications.

■ ASSOCIATED CONTENT

Supporting Information

The Supporting Information is available free of charge at https://pubs.acs.org/doi/10.1021/acs.langmuir.9b03542.

Materials, methods, characterization, Tables S1–4, and Figures S1–10 (PDF)

■ AUTHOR INFORMATION

Corresponding Author

*E-mail: kliu@jlu.edu.cn.

ORCID

Kun Liu: 0000-0003-2940-9814

Bai Yang: 0000-0002-3873-075X

Author Contributions

#Yu-Xi Wang, Ai-Ju Li, and He-Lei Wang contributed equally.

Notes

The authors declare no competing financial interest.

■ ACKNOWLEDGMENTS

K.L. thanks the National Natural Science Foundation of China (21674042, 21975094, and 21534004) for financial support. This work is also supported by program for JLU Science and Technology Innovative Research Team "JLUSTIRT2017TD-06" and the opening funds of State Key Laboratory of Applied

DOI: 10.1021/acs.langmuir.9b03542
Langmuir 2020, 36, 789–795

Optics, Changchun Institute of Optics, Fine Mechanics and Physics.

REFERENCES

(1) Sanchez, C.; Julian, B.; Belleville, P.; Popall, M. Applications of hybrid organic-inorganic nanocomposites. *J. Mater. Chem.* **2005**, *15*, 3559−3592.

(2) Kango, S.; Kalia, S.; Celli, A.; Njuguna, J.; Habibi, Y.; Kumar, R. Surface modification of inorganic nanoparticles for development of organic-inorganic nanocomposites—A review. *Prog. Polym. Sci.* **2013**, *38*, 1232−1261.

(3) Wang, S.; Kang, Y. F.; Wang, L. W.; Zhang, H. X.; Wang, Y. S.; Wang, Y. Organic/inorganic hybrid sensors: A review. *Sens. Actuators, B* **2013**, *182*, 467−481.

(4) Balazs, A. C.; Emrick, T.; Russell, T. P. Nanoparticle polymer composites: where two small worlds meet. *Science* **2006**, *314*, 1107−1110.

(5) Wang, K.; Jin, S.-M. M.; Xu, J.; Liang, R.; Shezad, K.; Xue, Z.; Xie, X.; Lee, E.; Zhu, J. Electric-Field-Assisted Assembly of Polymer-Tethered Gold Nanorods in Cylindrical Nanopores. *ACS Nano* **2016**, *10*, 4954−4960.

(6) Lv, H.; Sun, L.; Zou, L.; Xu, D.; Yao, H.; Liu, B. Size-dependent synthesis and catalytic activities of trimetallic PdAgCu mesoporous nanospheres in ethanol electrooxidation. *Chem. Sci.* **2019**, *10*, 1986−1993.

(7) Lv, H.; Sun, L.; Chen, X.; Xu, D.; Liu, B. One-step fabrication of trimetallic core−shell Au@ PdAuCu mesoporous nanospheres for ethanol electrooxidation. *Green Chem.* **2019**, *21*, 2043−2051.

(8) Wang, H.; Yao, L.; Mao, X.; Wang, K.; Zhu, L.; Zhu, J. Gold Nanoparticle Superlattice Monolayer with Tunable Interparticle Gap for Surface-Enhanced Raman Spectroscopy. *Nanoscale* **2019**, *11*, 13917−13923.

(9) Zhao, B.; Zhu, L. Mixed polymer brush-grafted particles: a new class of environmentally responsive nanostructured materials. *Macromolecules* **2009**, *42*, 9369−9383.

(10) Vaia, R. A.; Maguire, J. F. Polymer nanocomposites with prescribed morphology: going beyond nanoparticle-filled polymers. *Chem. Mater.* **2007**, *19*, 2736−2751.

(11) Chen, L.; Klok, H. A. "Multifaceted" polymer coated, gold nanoparticles. *Soft Matter* **2013**, *9*, 10678−10688.

(12) Corbierre, M. K.; Cameron, N. S.; Sutton, M.; Mochrie, S. G. J.; Lurio, L. B.; Rühm, A.; Lennox, R. B. Polymer-stabilized gold nanoparticles and their incorporation into polymer matrices. *J. Am. Chem. Soc.* **2001**, *123*, 10411−10412.

(13) Shan, J.; Tenhu, H. Recent advances in polymer protected gold nanoparticles: synthesis, properties and applications. *Chem. Commun.* **2007**, 4580−4598.

(14) Choueiri, R. M.; Galati, E.; Thérien-Aubin, H.; Klinkova, A.; Larin, E. M.; Querejeta-Fernández, A.; Han, L.; Xin, H. L.; Gang, O.; Zhulina, E. B.; Rubinstein, M.; Kumacheva, E. Surface patterning of nanoparticles with polymer patches. *Nature* **2016**, *538*, 79−83.

(15) Yan, N.; Liu, X.; Zhu, J.; Zhu, Y.; Jiang, W. Well-Ordered Inorganic Nanoparticle Arrays Directed by Block Copolymer Nanosheets. *ACS Nano* **2019**, *13*, 6638−6646.

(16) Galati, E.; Tebbe, M.; Querejeta-Fernández, A.; Xin, H.; Gang, O.; Zhulina, E. B.; Kumacheva, E. Shape-Specific Patterning of Polymer-Functionalized Nanoparticles. *ACS Nano* **2017**, *11*, 4995−5002.

(17) Liu, K.; Nie, Z. H.; Zhao, N.; Li, W.; Rubinstein, M.; Kumacheva, E. Step-growth polymerization of inorganic nanoparticles. *Science* **2010**, *329*, 197−200.

(18) Liu, Y.; Yang, X.; Huang, Z.; Huang, P.; Zhang, Y.; Deng, L.; Wang, Z.; Zhou, Z.; Liu, Y.; Kalish, H.; Khachab, N.; Chen, X.; Nie, Z. Magneto-Plasmonic Janus Vesicles for Magnetic Field-Enhanced Photoacoustic and Magnetic Resonance Imaging of Tumors. *Angew. Chem., Int. Ed.* **2016**, *55*, 15297−15300.

(19) Li, W.; Zhang, P.; Dai, M.; He, J.; Babu, T.; Xu, Y.-L.; Deng, R.; Liang, R.; Lu, M.-H.; Nie, Z.; Zhu, J. Ordering of gold nanorods in confined spaces by directed assembly. *Macromolecules* **2013**, *46*, 2241−2248.

(20) Bentz, K. C.; Savin, D. A. Chain Dispersity Effects on Brush Properties of Surface-Grafted Polycaprolactone-Modified Silica Nanoparticles: Unique Scaling Behavior in the Concentrated Polymer Brush Regime. *Macromolecules* **2017**, *50*, 5565−5573.

(21) Zhou, T.; Qi, H.; Han, L.; Barbash, D.; Li, C. Y. Towards controlled polymer brushes via a self-assembly-assisted-grafting-to approach. *Nat. Commun.* **2016**, *7*, 11119−11127.

(22) Flesch, C.; Delaite, C.; Dumas, P.; Bourgeat-Lami, E.; Duguet, E. Grafting of poly (ε-caprolactone) onto maghemite nanoparticles. *J. Polym. Sci., Part A: Polym. Chem.* **2004**, *42*, 6011−6020.

(23) Bissadi, G.; Weberskirch, R. Efficient synthesis of polyoxazoline-silica hybrid nanoparticles by using the "grafting-onto" approach. *Polym. Chem.* **2016**, *7*, 1271−1280.

(24) Oyerokun, F. T.; Vaia, R. A. Distribution in the grafting density of end-functionalized polymer chains adsorbed onto nanoparticle surfaces. *Macromolecules* **2012**, *45*, 7649−7659.

(25) Li, D. X.; He, Q.; Cui, X.; Li, J. B. Fabrication of pH-responsive nanocomposites of gold nanoparticles/poly (4-vinylpyridine). *Chem. Mater.* **2007**, *19*, 412−417.

(26) Krüger, C.; Agarwal, S.; Greiner, A. Stoichiometric functionalization of gold nanoparticles in solution through a free radical polymerization approach. *J. Am. Chem. Soc.* **2008**, *130*, 2710−2711.

(27) Chevigny, C.; Gigmes, D.; Bertin, D.; Jestin, J.; Boué, F. Polystyrene grafting from silica nanoparticles via nitroxide-mediated polymerization (NMP): synthesis and SANS analysis with the contrast variation method. *Soft Matter* **2009**, *5*, 3741−3753.

(28) Martinez, A. P.; Carrillo, J. M. Y.; Dobrynin, A. V.; Adamson, D. H. Distribution of chains in polymer brushes produced by a "grafting from" mechanism. *Macromolecules* **2016**, *49*, 547−553.

(29) El Harrak, A.; Carrot, G.; Oberdisse, J.; Jestin, J.; Boué, F. Atom transfer radical polymerization from silica nanoparticles using the 'grafting from'method and structural study via small-angle neutron scattering. *Polymer* **2005**, *46*, 1095−1104.

(30) Bartholome, C.; Beyou, E.; Bourgeat-Lami, E.; Chaumont, P.; Lefebvre, F.; Zydowicz, N. Nitroxide-mediated polymerization of styrene initiated from the surface of silica nanoparticles. In situ generation and grafting of alkoxyamine initiators. *Macromolecules* **2005**, *38*, 1099−1106.

(31) El Harrak, A.; Carrot, G.; Oberdisse, J.; Eychenne-Baron, C.; Boue, F. Surface- atom transfer radical polymerization from silica nanoparticles with controlled colloidal stability. *Macromolecules* **2004**, *37*, 6376−6384.

(32) Carrot, G.; Diamanti, S.; Manuszak, M.; Charleux, B.; Vairon, J. P. Atom transfer radical polymerization of n-butyl acrylate from silica nanoparticles. *J. Polym. Sci., Part A: Polym. Chem.* **2001**, *39*, 4294−4301.

(33) Joubert, M.; Delaite, C.; Bourgeat-Lami, E.; Dumas, P. Ring-opening polymerization of ε-caprolactone and L-lactide from silica nanoparticles surface. *J. Polym. Sci., Part A: Polym. Chem.* **2004**, *42*, 1976−1984.

(34) von-Werne, T.; Patten, T. E. Atom transfer radical polymerization from nanoparticles: a tool for the preparation of well-defined hybrid nanostructures and for understanding the chemistry of controlled/"living" radical polymerizations from surfaces. *J. Am. Chem. Soc.* **2001**, *123*, 7497−7505.

(35) Liu, Y.; Klep, V.; Zdyrko, B.; Luzinov, I. Polymer grafting via ATRP initiated from macroinitiator synthesized on surface. *Langmuir* **2004**, *20*, 6710−6718.

(36) Pyun, J.; Kowalewski, T.; Matyjaszewski, K. Synthesis of polymer brushes using atom transfer radical polymerization. *Macromol. Rapid Commun.* **2003**, *24*, 1043−1059.

(37) Kim, C. J.; Sondergeld, K.; Mazurowski, M.; Gallei, M.; Rehahn, M.; Spehr, T.; Frielinghaus, H.; Stühn, B. Synthesis and characterization of polystyrene chains on the surface of silica nanoparticles: Comparison of SANS, SAXS, and DLS results. *Colloid Polym. Sci.* **2013**, *291*, 2087−2099.

DOI: 10.1021/acs.langmuir.9b03542
Langmuir 2020, 36, 789−795

(38) Tom, J.; Ohno, K.; Perrier, S. Surface-initiated SET living radical polymerisation for the synthesis of silica-polymer core-shell nanoparticles. *Polym. Chem.* **2016**, *7*, 6075−6083.
(39) Carrot, G.; Rutot-Houzé, D.; Pottier, A.; Degée, P.; Hilborn, J.; Dubois, P. Surface-initiated ring-opening polymerization: A versatile method for nanoparticle ordering. *Macromolecules* **2002**, *35*, 8400−8404.
(40) Radhakrishnan, B.; Ranjan, R.; Brittain, W. J. Surface initiated polymerizations from silica nanoparticles. *Soft Matter* **2006**, *2*, 386−396.
(41) Alkilany, A. M.; Nagaria, P. K.; Wyatt, M. D.; Murphy, C. J. Cation exchange on the surface of gold nanorods with a polymerizable surfactant: polymerization, stability, and toxicity evaluation. *Langmuir* **2010**, *26*, 9328−9333.
(42) Kusolkamabot, K.; Sae-Ung, P.; Niamnont, N.; Wongravee, K.; Sukwattanasinitt, M.; Hoven, V. P. Poly (N-isopropylacrylamide)-stabilized gold nanoparticles in combination with tricationic branched phenylene-ethynylene fluorophore for protein identification. *Langmuir* **2013**, *29*, 12317−12327.
(43) Hansson, S.; Trouillet, V.; Tischer, T.; Goldmann, A. S.; Carlmark, A.; Barner-Kowollik, C.; Malmström, E. Grafting efficiency of synthetic polymers onto biomaterials: A comparative study of grafting-from versus grafting-to. *Biomacromolecules* **2013**, *14*, 64−74.
(44) Zhao, D.; Di Nicola, M.; Khani, M.; Jestin, J.; Benicewicz, B.; Kumar, S. Role of block copolymer adsorption versus bimodal grafting on nanoparticle self-assembly in polymer nanocomposites. *Soft Matter* **2016**, *12*, 7241−7247.
(45) Asai, M.; Zhao, D.; Kumar, S. K. Role of grafting mechanism on the polymer coverage and self-assembly of hairy nanoparticles. *ACS Nano* **2017**, *11*, 7028−7035.
(46) Smith, A. M.; Marbella, L. E.; Johnston, K. A.; Hartmann, M. J.; Crawford, S. E.; Kozycz, L. M.; Seferos, D. S.; Millstone, J. E. Quantitative analysis of thiolated ligand exchange on gold nanoparticles monitored by ^{1}H NMR spectroscopy. *Anal. Chem.* **2015**, *87*, 2771−2778.
(47) Jadhav, S. A.; Brunella, V.; Scalarone, D. Polymerizable ligands as stabilizers for nanoparticles. *Part. Part. Syst. Charact.* **2015**, *32*, 417−428.
(48) Hood, M. A.; Mari, M.; Muñoz-Espí, R. Synthetic strategies in the preparation of polymer/inorganic hybrid nanoparticles. *Materials* **2014**, *7*, 4057−4087.
(49) Corbierre, M. K.; Cameron, N. S.; Lennox, R. B. Polymer-stabilized gold nanoparticles with high grafting densities. *Langmuir* **2004**, *20*, 2867−2873.
(50) Shan, J.; Nuopponen, M.; Jiang, H.; Viitala, T.; Kauppinen, E.; Kontturi, K.; Tenhu, H. Amphiphilic gold nanoparticles grafted with poly (N-isopropylacrylamide) and polystyrene. *Macromolecules* **2005**, *38*, 2918−2926.
(51) Hussain, I.; Graham, S.; Wang, Z.; Tan, B.; Sherrington, D. C.; Rannard, S. P.; Cooper, A. I.; Brust, M. Size-controlled synthesis of near-monodisperse gold nanoparticles in the 1- 4 nm range using polymeric stabilizers. *J. Am. Chem. Soc.* **2005**, *127*, 16398−16399.
(52) Jin, L.; Liu, B.; Wang, P.; Yao, H.; Achola, L. A.; Kerns, P.; Lopes, A.; Yang, Y.; Ho, J.; Moewes, A.; Pei, Y.; He, J. Ultrasmall Au nanocatalysts supported on nitrided carbon for electrocatalytic CO 2 reduction: the role of the carbon support in high selectivity. *Nanoscale* **2018**, *10*, 14678−14686.
(53) Xia, Y. N.; Gilroy, K. D.; Peng, H. C.; Xia, X. H. Seed-Mediated Growth of Colloidal Nanocrystals. *Angew. Chem., Int. Ed.* **2017**, *56*, 60−95.
(54) Nikoobakht, B.; El-Sayed, M. A. Preparation and growth mechanism of gold nanorods (NRs) using seed-mediated growth method. *Chem. Mater.* **2003**, *15*, 1957−1962.
(55) Liu, K.; Zhao, N.; Kumacheva, E. Self-assembly of inorganic nanorods. *Chem. Soc. Rev.* **2011**, *40*, 656−671.
(56) Park, K.; Hsiao, M. S.; Koerner, H.; Jawaid, A.; Che, J.; Vaia, R. A. Optimizing seed aging for single crystal gold nanorod growth: the critical role of gold nanocluster crystal structure. *J. Phys. Chem. C* **2016**, *120*, 28235−28245.
(57) Corbierre, M. K.; Lennox, R. B. Preparation of thiol-capped gold nanoparticles by chemical reduction of soluble Au (I) - thiolates. *Chem. Mater.* **2005**, *17*, 5691−5696.
(58) Häkkinen, H. The gold-sulfur interface at the nanoscale. *Nat. Chem.* **2012**, *4*, 443−455.
(59) Xia, Y.; Xia, X.; Peng, H. C. Shape-controlled synthesis of colloidal metal nanocrystals: thermodynamic versus kinetic products. *J. Am. Chem. Soc.* **2015**, *137*, 7947−7966.
(60) Odian, G. *Principles of Polymerization*, 4th ed.; John Wiley & Sons: Hoboken, NJ, 2004; pp 42, 729.
(61) Huang, X.; Neretina, S.; El-Sayed, M. A. Gold nanorods: from synthesis and properties to biological and biomedical applications. *Adv. Mater.* **2009**, *21*, 4880−4910.

DOI: 10.1021/acs.langmuir.9b03542
Langmuir 2020, 36, 789−795